*Inorg. Chem.* **2007**, *46*, 10670–10680

# Ionothermal Syntheses of Six Three-Dimensional Zinc Metal–Organic Frameworks with 1-Alkyl-3-methylimidazolium Bromide Ionic Liquids as Solvents

**Ling Xu,[†] Eun-Young Choi,[‡] and Young-Uk Kwon*[,†,‡,§]**

*Department of Chemistry, BK-21 School of Chemical Materials Sciences, Sungkyunkwan University, Suwon, 440-176 Korea, Institute of Basic Science, Sungkyunkwan University, Suwon, 440-176 Korea, and SKKU Advanced Institute of Nanotechnology, Sungkyunkwan University, Suwon, 440-176 Korea*

Received July 13, 2007

We have performed ionothermal reactions between $Zn(NO_3)_2$ and $H_3BTC$ in 1-alkyl-3-methylimidazolium bromide ionic liquids with the alkyl group varying from ethyl to amyl. Six 3-D metal–organic frameworks (MOFs), including two isomeric compounds $[Zn_3(BTC)_2(H_2O)_2]\cdot 2H_2O$ (**1** and **2**) ($H_3BTC$ = 1,3,5-benzenetricarboxylate acid), [EMI][Zn(BTC)] (**3**) (E = ethyl, MI = 3-methylimidazolium), [PMI][Zn(BTC)](**4**) (P = propyl), $[BMI]_2[Zn_4(BTC)_3(OH)(H_2O)_3]$ (**5**) (B = butyl), and [AMI][$Zn_2$(BTC)(OH)Br] (**6**) (A = amyl), have been synthesized and structurally characterized. Compounds **1** and **2** are isomeric compounds, in which the coordination modes of Zn atoms and the $BTC^{3-}$ ligands are considerably different. Compounds **3**–**6** crystallize with the corresponding ionic liquid cations incorporated in the frameworks. Their crystal structures show various features including various coordination geometries of $Zn^{2+}$ and various bridging modes of the $BTC^{3-}$ ligands. The incorporated cations appear to have strong interactions with the frameworks.

## Introduction

Ionothermal synthesis is a novel material synthesis method,[1−3] in which ionic liquids (ILs) function as reaction media, templates, or charge-compensating groups. ILs have many intriguing characteristic physicochemical properties such as high ionic conductivity, nonflammability, and negligible vapor pressure.[4] The coexistence of ionic and organic groups and the large temperature windows of ILs make them ideal media for the reactions between metal ions and organic ligands. With these attributes, ionothermal synthesis is considered to be more environment-friendly and safer than the traditional hydro/solvothermal reactions, which are frequently used in the exploratory syntheses of inorganic and inorganic−organic hybrid materials. In addition, ionothermal solvent systems can provide different reaction conditions from those of hydro/solvothermal systems, by which novel structure types such as zeolite and zeo-type frameworks can be obtained.[2,3a,b,5]

There are a number of examples in which ILs have been successfully applied to the syntheses of novel metal−organic frameworks (MOFs).[6] Since the physical properties of ILs can be tailored, it follows naturally to explore ionothermal MOF synthesis systems by employing ILs that are systematically varied in structure. One such variation is the length of the alkyl group on the imidazolium cation. With the increase of the alkyl chain length, the viscosity of the IL increases and the melting point decreases, although such a trend is reverted when there are more than seven carbons in the alkyl chain.[7,8]

* Corresponding author. E-mail: ywkwon@skku.edu.
[†] Department of Chemistry.
[‡] Institute of Basic Science.
[§] SKKU Advanced Institute of Nanotechnology.

(1) Wasserscheid, P.; Keim, W. *Angew. Chem., Int. Ed.* **2000**, *39*, 3772−3789.
(2) Copper, E. R.; Andrew, C. D.; Wheatley, P. S.; Webb, P. B.; Wormald, P.; Morris, R. E. *Nature*. **2004**, *430*, 1012−1016.
(3) (a) Parnham, E. R.; Wheatley, P. S.; Morris, R. E. *Chem. Commun*. **2006**, 380−382. (b) Parnham, E. R.; Morris, R. E. *J. Am. Chem. Soc*. **2006**, *128*, 2204−2205. (c) Xu, Y. P.; Tian, Z. J.; Wang, S. J.; Hu, Y.; Wang, L.; Wang, B. C.; Ma, Y. C.; Hou, L.; Yu, J. Y.; Lin, L. W. *Angew. Chem., Int. Ed*. **2006**, *45*, 3965−3970.
(4) (a) Camper, D.; Scovazzo, P.; Koval, C.; Noble, R. *Ind. Eng. Chem. Res*. **2004**, *43*, 3049−3054. (b) Gutowski, K. E.; Broker, G. A.; Willauer, H. D.; Huddleston, J. G.; Swatloski, R. P.; Holbrey, J. D.; Rogers, R. D. *J. Am. Chem. Soc*. **2003**, *125*, 6632−6633. (c) Hoffmann, J.; Nuchter, M.; Ondruschka, B.; Wasserscheid, P. *Green Chem*. **2003**, *5*, 296−299.
(5) (a) Parnham, E. R.; Morris, R. E. *Chem. Mater*. **2006**, *18*, 4882−4887. (b) Parnham, E. R.; Morris, R. E. *J. Mater. Chem*. **2006**, *16*, 3682−3684.



10.1021/ic701393w CCC: $37.00 
Published on Web 11/15/2007

**Table 1.** Main IR Characteristic Absorption Peaks for Compounds **1**−**6**

| compd | $\upsilon_{as}(COO^-)$, $cm^{-1}$ | $\upsilon_s(COO^-)$, $cm^{-1}$ | $\delta$(C−H)(MI), $cm^{-1}$ | $\delta$(C−N)(MI), $cm^{-1}$ | $\delta$(C−H), $cm^{-1}$ |
|---|---|---|---|---|---|
| **1** | 1630, 1565 | 1437, 1362 | | | 2980, 2924 |
| **2** | 1626, 1575 | 1446, 1379 | | | 2973, 2923 |
| **3** | 1630, 1565 | 1438, 1350 | 3150, 3066 | 1160 | 2973, 2930 |
| **4** | 1612, 1560 | 1430, 1365 | 3147, 3097 | 1164 | 2972, 2890 |
| **5** | 1633, 1536 | 1455, 1385 | 3117, 3041 | 1156 | 2974, 2890 |
| **6** | 1625, 1567 | 1446, 1379 | 3156, 3076 | 1162 | 2974, 2893 |

In the present study, we synthesized and used four sorts of 1-alkyl-3-methylimidazolium bromide ILs with different alkyl chain lengths from two to five carbons, (1-ethyl-3-methylimidazolium bromide ([EMI]Br), 1-propyl-3-methylimidazolium bromide ([PMI]Br), 1-butyl-3-methylimidazolium bromide ([BMI]Br), and 1-amyl-3-methylimidazolium bromide ([AMI]Br), as solvents. In order to isolate the effects of the variation on the cation part, we have fixed all the other variables such as the anion of ILs, the types of reagent metal ion, and ligand. In the present paper, the anion is $Br^-$ and metal ion is $Zn^{2+}$. An aromatic rigid polycarboxylic acid, 1,3,5-benzenetricarboxylic acid ($H_3BTC$), a versatile and powerful ligand with its three carboxylate groups as short bridges and a benzene ring as a long bridge between metal centers leading to structural varieties, is chosen as the ligand. In fact, this Zn−BTC system is one of the most extensively explored systems in the endeavor for synthesizing novel MOFs[9,10] While many different solvent systems and reaction techniques have been used, there is not a single case of Zn−BTC system under ionothermal conditions reported in the literature. Surprisingly, our results reveal that the ionothermal reaction technique is extremely versatile in producing many new MOFs with some new features. Herein, the syntheses and crystal structures of six novel 3-D Zn−BTC MOFs, $[Zn_3(BTC)_2(H_2O)_2]\cdot 2H_2O$ (**1** and **2**), [EMI][Zn(BTC)] (**3**), [PMI][Zn(BTC)](**4**), $[BMI]_2[Zn_4(BTC)_3(OH)(H_2O)_3]$ (**5**), and [AMI]$[Zn_2(BTC)(OH)Br]$ (**6**), are presented.

## Experiment Section

**Syntheses of the Compounds.** All chemicals were commercially purchased and used without further purification. The ILs were prepared according to the literature method.[11,5a] Under inert nitrogen atmosphere conditions, degassed alkyl bromide was refluxed with the distilled 1-methylimidazole to give the corresponding ILs. The four sorts of ILs were washed with ethyl acetate and then dried under a vacuum at least for 10 h: [EMI]Br (white solid, mp = 80−82 °C, yield: 92%), [PMI]Br (pale yellow oil, yield: 80%), [BMI]Br (pale yellow oil, yield: 78%), [AMI]Br (pale brown oil, yield: 68%).

**$[Zn_3(BTC)_2(H_2O)_2]\cdot 2H_2O$ (1 and 2).** $Zn(NO_3)_2\cdot 6H_2O$ (1.5 mmol, 0.446 g for **1**; 2.0 mmol, 0.595 g for **2**) and $H_3BTC$ (0.5 mmol, 0.105 g) were placed in a 25 mL Teflon-lined stainless-steel autoclave mixed with [EMI]Br (1.0 g). The mixtures were kept in a furnace at 160 °C for 5 days and then naturally cooled to room temperature to get colorless crystals of **1** and **2** suitable for X-ray diffraction. Yield for **1**, 69%, for **2**, 72% (based on $H_3BTC$). Elemental analysis found (calcd) for **1**: C, 31.59(31.68); H, 2.13(2.07); for **2**: C, 31.72(31.68); H, 1.96(2.07). IR data (in KBr, $cm^{-1}$) for **1**: 3423(s), 2980(m), 2924(m), 2358(m), 1630(s), 1565(s), 1500(m), 1437(m), 1362(s), 1101(m), 731(w), 615(w), 574(w), 460(w); for **2**: 3419(vs), 2973(w), 2923(m), 1626(vs), 1575(s), 1485(w), 1446(s), 1379(s), 1051(w), 719(w), 649(w), 568(w), 463(w).


(6) (a) Jin, K.; Huang, X. Y.; Pang, L.; Li, J.; Appel, A.; Wherland, S. *Chem. Commun*. **2002**, 2872−2873. (b) Danil, N. D.; Chun, H. C.; Kim, K. M. *Chem. Commun*. **2004**, 1594−1595. (c) Lin, Z. J.; Wragg, D. S.; Morris, R. E. *Chem. Commun.* **2006**, 2021−2023. (d) Liao, J. H.; Wu, P. C.; Huang, W. C. *Cryst. Growth Des.* **2006**, *6*, 1062−1063. (e) Sheu, C. Y.; Lee, S. F.; Lii, K. H. *Inorg. Chem*. **2006**, *45*, 1891−1893. (f) Tsao, C. P.; Sheu, C. Y.; Nguyen, N.; Lii, K. H. *Inorg. Chem*. **2006**, *45*, 6361−6364. (g) Liao, J. H.; Huang, W. C. *Inorg. Chem. Commun*. **2006**, *9*, 1227−1231. (h) Lin, Z. J.; Slawin, A. M. Z.; Morris, R. E. *J. Am. Chem. Soc.* **2007**, *129*, 4880−4881. (f) Parnham, E. R.; Morris, R. E. *Acc. Chem. Res.* **2007**, in press. (DOI: 10.1021/ar 700025K). (g) Lin, Z.; Wragg, J. E.; Morris, R. E. *J. Am. Chem. Soc.* **2007**, *129*, 10334−10335.

(7) (a) Holbrey, J. D.; Seddon, K. R. *J. Chem. Soc., Dalton Trans*. **1999**, 2133−2140. (b) Larsen, A. S.; Holbrey, J. D.; Tham, F. S.; Reed, C. A. *J. Am. Chem. Soc*. **2000**, *122*, 7264−7272.

(8) (a) Wasserscheid, P.; Welton, T. *Ionic Liquids in Synthesis*; Wiley-VCH: Weinehim, Germany, 2003; Chapter 3. (b) Tokuda, H.; Hayamizu, K.; Ishii, K.; Susan, M.; Watanabe, M. *J. Phys. Chem. B* **2005**, *109*, 6103−6110.

(9) (a) Robl, C. *Z. Anorg. Allg. Chem.* **1988**, *561*, 57−65. (b) Yaghi, O. M.; Li, G.; Li, H. *Chem. Mater*. **1997**, *9*, 1074−1076. (c) Yaghi, O. M.; Davis, C. E.; Li, G. M.; Li, H. L. *J. Am. Chem. Soc*. **1997**, *119*, 2861−2868. (d) Plater, M. J.; Foreman, M. R. St. J.; Coronado, E.; Gomez-Garcia, C. J.; Slawin, A. M. Z. *J. Chem. Soc., Dalton Trans.* **1999**, 4209−4216. (e) Plater, M. J.; Foreman, M. R St J.; Howie, R. A.; Skakle, J. M. S.; Coronado, E.; Gomez-Garcia, C. J.; Gelbrich, T.; Hursthouse, M. B. *Inorg. Chim. Acta* **2001**, *319*, 159−175. (f) Kim, J. H.; Chen, B. L.; Reineke, T. M.; Li, H. L.; Eddaoudi, M.; Moler, D. B.; O'Keeffe, M.; Yaghi, O. M. *J. Am. Chem. Soc.* **2001**, *123*, 8239−8247. (g) Shi, Z.; Hou, Y.; Hua, J.; Li, G.; Feng, S. *Acta Crystallogr., Sect. C: Cryst. Struct. Commun.* **2003**, *59*, m337. (h) Krishnamurthy, D.; Murugavel, R. *Indian J. Chem., Sect. A: Inorg., Bioinorg., Phys. Theor. Anal. Chem.* **2003**, *42*, 2267. (i) Chen, W.; Wang, J. Y.; Chen, C.; Yue, Q.; Yuan, H. M.; Chen, J. S.; Wang, S. N. *Inorg. Chem*. **2003**, *42*, 944−946. (j) Li, X.; Sun, D.; Cao, R.; Sun, Y.; Wang, Y.; Bi, W.; Gao, S.; Hong, M. *Inorg. Chem. Commun.* **2003**, *6*, 908−911. (k) Wu, G.; Shi, X.; Fang, Q. R.; Tian, G.; Wang, L. F.; Zhu, G. S.; Addison, A. W.; Wei, Y.; Qiu, S. F. *Inorg. Chem. Commun.* **2003**, *6*, 402−404.

(10) (a) Shi, Z.; Li, G.; Wang, L.; Gao, L.; Chen, X.; Hua, J.; Feng, S. *Cryst. Growth Des.* **2004**, *4*, 25−27. (b) Li, X.; Cao, R.; Sun, D.; Yuan, D.; Bi, W.; Li, X.; Wang, Y. *J. Mol . Struct.* **2004**, *694*, 205−210. (c) Zhou, Y. F.; Lou, B. Y.; Yuan, D. Q.; Xu, Y. Q.; Jiang, F. L.; Hong, M. C. *Inorg. Chim. Acta* **2005**, *358*, 3057−3064. (d) Majumder, A.; Shit, S.; Choudhury, C. R.; Batten, S. R.; Pilet, G.; Luneau, D.; Daro, N.; Sutter, J. P.; Chattopadhyay, N.; Mitra, S. *Inorg. Chim. Acta* **2005**, *358*, 3855−3864. (e) Jo, H. J.; Lough, A. J.; Kim, J. C. *Inorg. Chin. Acta* **2005**, *358*, 1274−1278. (f) Xie, L.; Liu, S.; Gao, B.; Zhang, C.; Sun, C.; Li, D.; Su, Z. *Chem. Commun.* **2005**, 2402−2404. (g) Zhao, X. J.; Tao, J. *Appl. Organomet. Chem.* **2005**, *19*, 694−695. (h) Wang, Z.; Kravtsov, V. C.; Zaworotko, M. J. *Angew. Chem., Int. Ed.* **2005**, *44*, 2877−2880. (i) He, J.; Zhang, Y.; Pan, Q.; Yu, J.; Ding, H.; Xu, R. *Microporous Mesoporous Mater*. **2006**, *90*, 145−152. (j) Fang, Q.; Zhu, G.; Xue, M.; Sun, J.; Sun, F.; Qiu, S. *Inorg. Chem*. **2006**, *45*, 3582−3587. (k) Du, M.; Jiang, X. J.; Zhao, X. J. *Inorg. Chem.* **2006**, *45*, 3998−4006. (l) Luo, F.; Che, Y. X.; Zheng, J. M. *Inorg. Chem. Commun.* **2006**, *9*, 1045−1048. (m) Zhang, J.; Chen, Y. B.; Chen, S. M.; Li, Z. J.; Cheng, J. K.; Yao, Y. G. *Inorg. Chem*. **2006**, *45*, 3161−3163. (n) Braverman, M. A.; Supkowski, R. M.; LaDuca, R. L. *J. Solid. State Chem.* **2007**, *180*, 1852−1862. (o) Liu, Y. Y.; Ma, J. F.; Yang, J.; Su, Z. M. *Inorg. Chem*. **2007**, *46*, 3027−3037. (p) Xiao, D. R.; Wang, E. B.; An, H. Y.; Li, Y. G.; Xu, L. *Cryst. Growth Des*. **2007**, *7*, 506−512.

(11) Bonhote, P.; Dias, A. P.; Papageorgiou, N.; Kalyanasundaram, K.; Cratzel, M. *Inorg. Chem*. **1996**, *35*, 1168−1178.

**Table 2.** Factors Affecting the Reaction System and Resulting MOFs

| compd | ionic liquid | coordination modes of $BTC^{3-}$ | connectivity modes of $BTC^{3-}$ in Scheme 1 | stoichiometry of $n_{Zn}:n_{BTC}^{3-}$ | coordination geometries of Zn |
|---|---|---|---|---|---|
| $[Zn_3(BTC)_2(H_2O)_2]\cdot 2H_2O$ (**1**) | [EMI]Br | bridging monodentate and bis-didentate | A | 1.5:0.5 | 6, 4 |
| $[Zn_3(BTC)_2(H_2O)_2]\cdot 2H_2O$ (**2**) | [EMI]Br | chelating/bridging bidentate and bis-bidentate | B | 2.0:0.5 | 6, 5 |
| [EMI][Zn(BTC)] (**3**) | [EMI]Br | bidentate and bis-monodentate | F | 3.0:0.5 | 4 |
| [PMI][Zn(BTC)] (**4**) | [PMI]Br | tri-monodentate | H | 1.5:0.5 | 3 |
| $[BMI]_2[Zn_4(BTC)_3(OH)(H_2O)_3]$ (**5**) | [BMI]Br | tri-monodentate and tri-bidentate | C, H | 2.0:0.5 | 4, 4, 6, 4 |
| [AMI][$Zn_2$(BTC)(OH)Br] (**6**) | [AMI]Br | monodentate and bis-bidentate | D | 3.5:0.5 | 5, 4 |

**[EMI][Zn(BTC)] (3)**. $Zn(NO_3)_2\cdot 6H_2O$ (3.0 mmol, 0.893 g) and $H_3BTC$ (0.5 mmol, 0.105 g), were mixed with 1.0 g [EMI]Br in a 25 mL Teflon-lined stainless-steel autoclave. The mixture was heated at 160 °C for 5 days in a furnace to obtain colorless crystals of **3**. Yield: 70% (based on $H_3BTC$). Elemental analysis found (calcd): C, 46.91(46.96); H, 3.36(3.68); N, 7.16(7.30). IR data (in KBr, $cm^{-1}$): 3420(w), 3150(m), 3066(m), 2973(m), 2930(m), 1630(s), 1565(s), 1438(s), 1350(s), 1160(s), 834(w), 764(s), 725(s), 538(m), 446(m).

**[PMI][Zn(BTC)](4)**. A mixture of $Zn(NO_3)_2\cdot 6H_2O$ (1.5 mmol, 0.446 g), $H_3BTC$ (0.5 mmol, 0.105 g), and [PMI]Br (1.0 mL) in a 25 mL Teflon-lined stainless-steel autoclave was heated to 160 °C for 5 days in a furnace. The resulting mixture was naturally cooled until colorless crystals of **4** obtained. Yield: 60% (based on $H_3BTC$). Elemental analysis found (calcd): C, 48.45(48.32); H, 3.97(4.06); N, 6.95(7.04). IR data (in KBr, $cm^{-1}$): 3425(s), 3147(w), 3097(w), 2972(w), 2890(w), 1612(s), 1560(s), 1430(w), 1384(s), 1365(s), 1164(w), 1051(s), 879(w), 725(w), 536(w), 463(w).

**$[BMI]_2[Zn_4(BTC)_3(OH)(H_2O)_3]$ (5)**. $Zn(NO_3)_2\cdot 6H_2O$ (2.0 mmol, 0.595 g) and $H_3BTC$ (0.5 mmol, 0.105 g) were mixed with [BMI]Br (1.0 mL) in a 25 mL Teflon-lined stainless-steel autoclave and then heated to 160 °C for 5 days. The mixture was naturally cooled to get colorless crystals of **5**. Yield: 70% (based on $H_3BTC$). Elemental analysis found (calcd): C, 41.09(40.92); H, 3.68(3.43); N, 4.44(4.66). IR data (in KBr, $cm^{-1}$): 3423(vs), 3117(w), 3041(w), 2974(s), 2890(w), 1633(s), 1536(w), 1455(s), 1385(s), 1325(w), 1269(w), 1156(w), 1051(s), 881(w), 600(w), 436(w).

**[AMI][$Zn_2$(BTC)(OH)Br] (6)**. $Zn(NO_3)_2\cdot 6H_2O$ (3.5 mmol, 1.041 g), $H_3BTC$ (0.5 mmol, 0.105 g), and [AMI]Br (1.0 mL) were heated at 160 °C for 5 days in a 25 mL Teflon-lined stainless-steel autoclave in a furnace. Colorless crystals of **6** resulted from the natural cooling. Yield: 75% (based on $H_3BTC$). Elemental analysis found (calcd): C, 36.71(36.83); H, 3.68(3.43); N, 4.71(4.77). IR data (in KBr, $cm^{-1}$): 3419(s), 3156(s), 3124(s), 3096(s), 3076(s), 2974(s), 2893(w), 1625(s), 1567(s), 1446(s), 1379(s), 1162(s), 1051(s), 935(s), 719(s), 624(w), 583(w), 551(w), 487(s), 463(w).

**Characterizations.** Thermogravimetric (TG) analyses were carried on a TA4000/SDT 2960 instrument in flowing $N_2$ with a heating rate of 10 °C·$min^{-1}$. TG data of the six compounds show that they have high thermal stabilities. The weight losses in compounds **1**, **3**, **4**, and **6** occur in single steps, while **2** and **5** show two-step weight losses with the first ones corresponding to water losses (Supporting Information; Figure S1).

Crystallographic data were collected at −100 °C for **1** and 25 °C for the others on Bruker CCD diffractiometers in different locations including Korea Basic Science Institute. The structures were solved by the direct methods using SHELXTL package of crystallographic software[12] and refined by the full-matrix least-squares technique on $F^2$. All non-hydrogen atoms were refined anisotropically, and the hydrogen atoms were included in the final stages of the refinements on calculated positions bonded to their carrier atoms.

X-ray powder diffraction (XRPD) data were recorded on a Rigaku D/max-RC diffractometer with Cu Kα radiation ($\lambda = 1.5406$ Å, 30 kV, and 40 mA) with a scan speed of 2° $min^{-1}$ and a step size of 0.02° in $2\theta$. The experimental XRPD patterns for compounds **1** to **6** match well with those simulated from single-crystal structure data (Supporting Information; Figure S2), indicating that all six compounds were isolated as single phases.

Elemental analysis (C, H, and N) was performed on an EA1110 elemental analyzer, and the data compared experiment with calculation, confirming the single phases of six compounds.

FT-IR spectra were obtained on a Bruker Tensor27 FT-IR spectrometer using KBr pellets dispersed with sample powders in the range of 4000−400 $cm^{-1}$. The characteristic absorption peaks of the main functional groups for **1**−**6** are listed in Table 1. The asymmetric stretching vibrations $\nu_{as}(COO^-)$ were observed in the rang 1536−1633 $cm^{-1}$ and symmetric stretching vibrations $\nu_s(COO^-)$ in 1350−1455 $cm^{-1}$. The above stretching was shifted to lower values, compared to the carbonyl frequencies of free $H_3BTC$ ligand. The difference $\Delta(\nu_{as}(COO^-) - \nu_s(COO^-))$ were around 200 $cm^{-1}$, characteristic for coordinated carboxylate groups.[13] The peaks for **1**−**6** from 2890 to 2980 $cm^{-1}$ are from C−H stretching vibrations.[14] The peaks for **3**−**6** around 1160 $cm^{-1}$ can be assigned as $N_{alkyl}$−C stretching of the imidazolium rings.[15]

## Results and Discussion

Each of the compounds **1**−**6** was obtained as a single phase product under the conditions given in the Experimental Section. Compounds **1**−**3** were obtained from the reactions between $Zn^{2+}$ and $BTC^{3-}$ in a [EMI]Br medium. The only difference among their synthesis conditions is the different Zn/$H_3BTC$ ratios (Table 2). Remarkably, the crystal structural data reveal that the variation of starting composition is

(12) Sheldrick, G. M. *SHELXTL Programs, Version 5.1*; Bruker AXS GmbH; Karlsruhe, Germany, 1998.
(13) (a) Nakamoto, K. *Infrared Spectra of Inorganic and Coordination Compounds*;Wiley:New York, 1986. (b) Deacon, G. B.; Philips, R. *J. Coord. Chem. Rev.* **1980**, *33*, 227−250. (c) Djordjevic, C.; Lee, M.; Sinn, E. *Inorg. Chem.* **1989**, *28*, 719−723.
(14) (a) Hitchcock, P. B.; Seddon, K. R.; Welton, T. *J. Chem. Soc., Dalton Trans.***1993**, 2639−2643. (b) Elaiwi, A.; Hitchcock, P. B.; Seddon, K. R.; Srinicasan, N.; Tan, Y. M.; Welton, T.; Zora, J. A. *J. Chem. Soc., Dalton Trans*. **1995**, 3467−3471.
(15) (a) Koel, M.; Porc, E. *Acad. Sci. Chem*. **2000**, *49*, 145−155. (b) Katsyuba, S. A.; Dyson, P. J.; Vandyukova, E. E.; Chernova, A. V.; Vidis, A. *Helv. Chim. Acta* **2004**, *87*, 2556−2565.

**Scheme 1.** Connectivity Modes of BTC Ligands with Zn Found in the Literatures on Zn−BTC MOFs and the Crystal Structures of the Present Paper

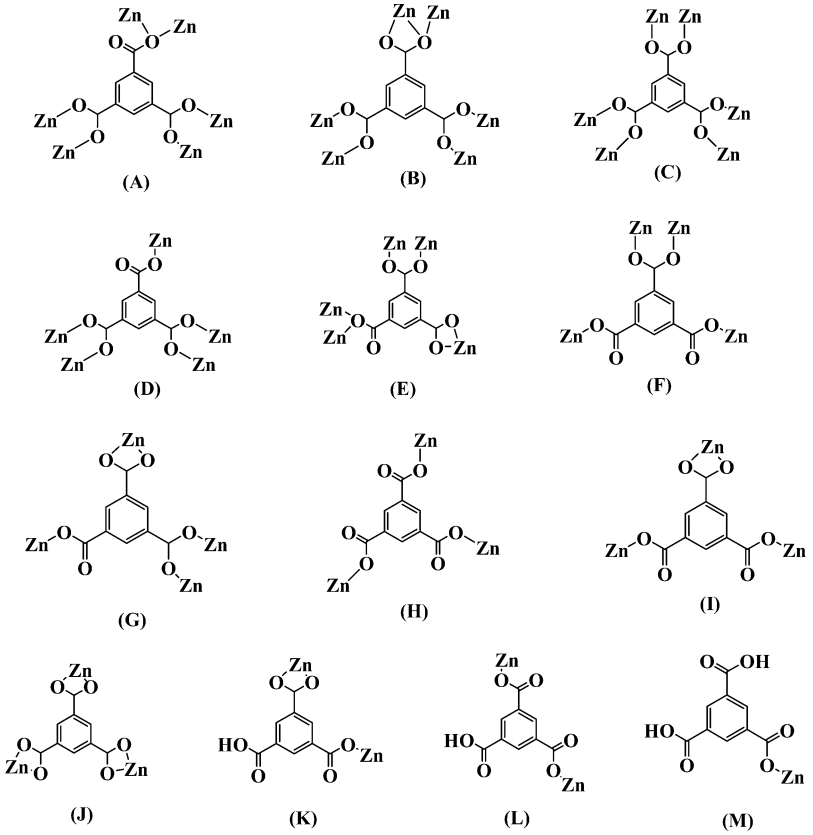


significant enough to result in totally different compounds. As will be discussed below, **1** and **2** are free of template, while **3** is formed with $EMI^+$ as a template. The other compounds **4**−**6** were obtained from the reactions between $Zn^{2+}$ and $H_3BTC$ in IL media with longer alkyl chains and were constituted with the corresponding organic cations incorporated. All of the crystal structures of compounds **1**−**6** can be described as 3-D frameworks constructed by connecting $Zn^{2+}$ atoms and $BTC^{3-}$ ligands in various modes and various ratios.

It seems appropriate to briefly overview the structures of Zn−BTC MOFs in the literatures before discussing on the details of our compounds.[9,10] There are 41 different Zn−BTC MOFs reported until now. These structures can be classified into 11 different types of connectivity modes around the BTC ligand. Each of compounds **1** and **2** shows yet a new mode to make total of 13 types of connectivity modes of BTC with Zn, which are shown in Scheme 1. In this scheme, the modes are arranges in the order of decreasing number of Zn atoms bonded to a BTC from six to one. Mode L with two Zn atoms is the most frequently found with ten examples, followed by mode H (with three Zn) and mode F (with four Zn) each with seven examples. Modes C (with six Zn) and D (with five Zn) are also found in five cases each (Supporting Information; Table S1). The 13 modes span all of the possible features of bonds between a carboxylic group and a Zn atom (or Zn atoms). For example, there are protonated and deprotonated carboxylic groups, there are monodentate and bidentate carboxylic groups bonded to a Zn, and there are $\mu_2$-oxo bridges and $\mu_2$-carboxylic bridges between two Zn ions.

According to Scheme 1, the connectivity modes of BTCs found in **1**−**6** are A (in **1**), B (**2**), C (**5**), D (**6**), F (**3**), and H (**4** and **5**). It is noteworthy that BTCs in **1**−**6** tend to be bonded to large numbers of Zn atoms of from four to six (Scheme 1). While **1** and **2** have unique connectivity modes, **3**, **4**, **5**, and **6** show popular ones each of which appeared five through nine times from the 41 Zn−BTC MOFs in the literature.

It needs to be emphasized that the connectivity modes in compounds **1** and **2** have not been reported despite that Zn−BTC systems have been studied extensively. This probably has something to do with the solvent systems used for the syntheses. To the best of our knowledge, this is the first time to present Zn−BTC coordination polymers synthesized in IL systems. Probably the unique properties of ILs as solvents, i.e., the large dielectric constant and the high viscosity, as well as the possibility to function as templates, affect the reactions and reinforce new structures. Therefore, even if ionic liquid is not incorporated in the final frameworks for compounds **1** and **2** (unlike **3**, **4**, **5**, and **6** which contain the cations of the ILs) these compounds show some new features such as the new connectivity modes of BTC.

**Description of Crystal Structures 1−6.** The structure of **1** features a 3-D framework in which the $BTC^{3-}$ ligand exhibits a $\mu_6$ coordination mode: three carboxylate groups adopt bridging monodentate and bis-bidentate coordination fashion (mode A in Scheme 1). As shown in Figure 1a, Zn-

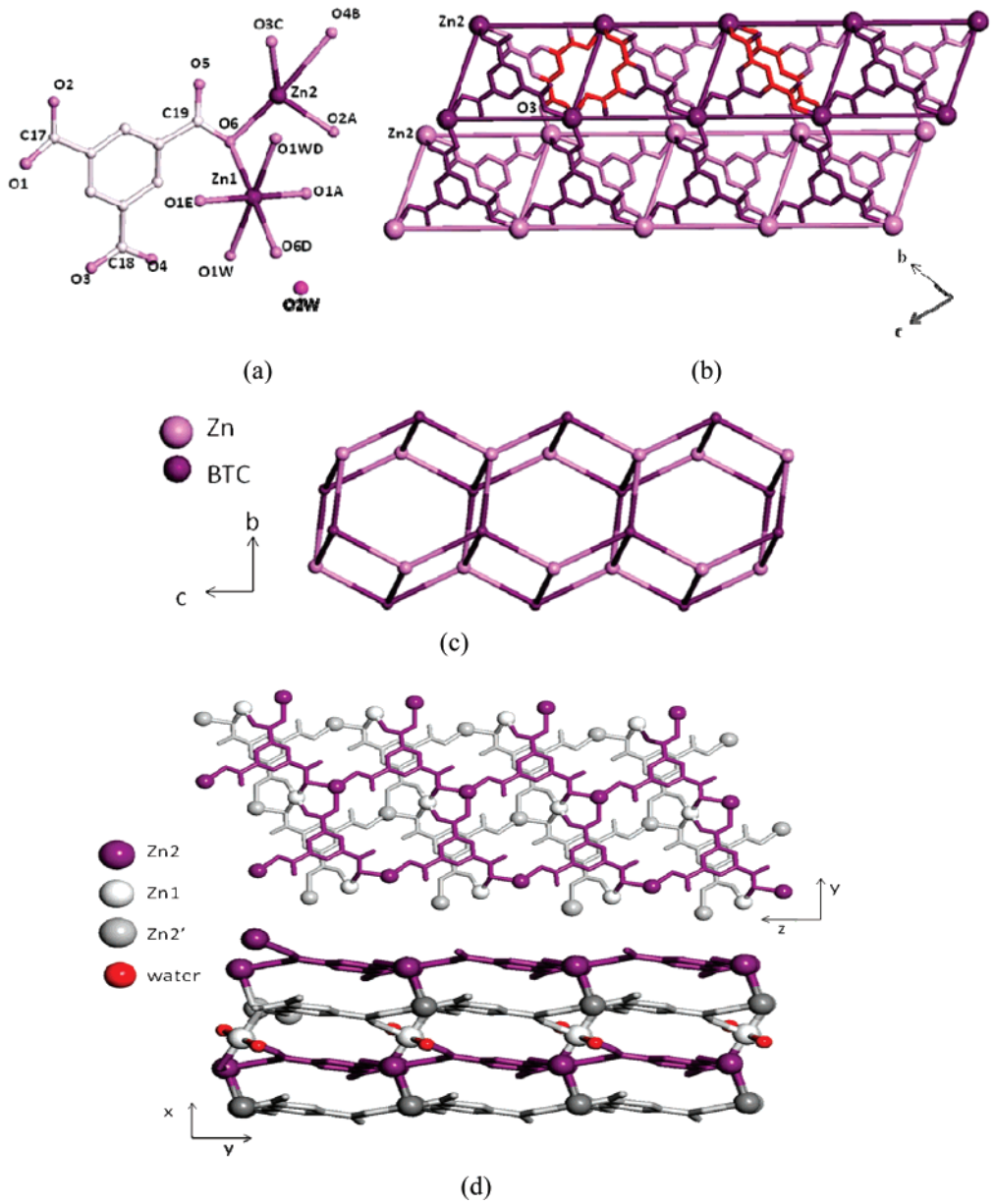


**Figure 1.** Structure of **1**: (a) Coordination environment of Zn. (b) The 2-D layer formed by linking the $[(Zn2)_4(BTC)_2]$ units with the water molecules being omitted for clarity. (c) The topological drawing of 2-D layer. (d) 3-D framework.

(1) atom is in an octahedral geometry constructed by four carboxylic oxygen atoms ($d_{Zn(1)-O} = 2.160(2)-2.310(2)$ Å) in the equatorial positions and two symmetry-related water molecules in the axial positions ($d_{Zn(1)-O(1W)} = 2.467(2)$ Å). Zn(2) center is coordinated by four carboxylic oxygen atoms from four $BTC^{3-}$ ligands to form a distorted tetrahedral geometry ($d_{Zn(2)-O} = 2.191(1)-2.342(2)$ Å). $BTC^{3-}$ ligands are paired with the phenyl rings parallel to each other, and they are connected to four Zn(2) atoms to form two kinds of 16-membered rings $[Zn_2(BTC)_2]$; the expansion of such units produces a ladder-like chain along the *b*-direction. The ladders so generated are further connected to the next ones through the linkage between O(3) and Zn(2) into a 2-D layer along the *bc* plane (Figure 1b) with a distance of 9.879 Å between the ladders. The 2-D layer is connected to the next ones through $Zn(1)O_4$ tetrahedral bridges to form a 3-D framework structure (Figure 1d). Water molecules O(2W) are stabilized in the framework by hydrogen bonds with carboxylic oxygen atoms (O(2W)···O(3) = 2.984(3) Å; O(2W)···O(5) = 2.933(3) Å). The centroid-to-centroid distance of 3.808 Å between the paired phenyl rings of $BTC^{3-}$ ligands indicate the existence of a weak $\pi\cdots\pi$ stacking interaction.

**2** has the same composition as **1** and is also a 3-D framework structure. However, as mentioned earlier, they show different connectivity modes, which, in turn, make the two structures different in many aspects. The $BTC^{3-}$ ligand in **2** shows the connectivity mode B in Scheme 1 and is bonded to six Zn atoms in a chelating/bridging bidentate and bis-bidentate fashion. The coordination environment of Zn-(1) atom is an octahedron ($d_{Zn(1)-O} = 2.025(1)-2.144(2)$ Å), similar to that of Zn(1) in **1**. However, Zn(2) is surrounded

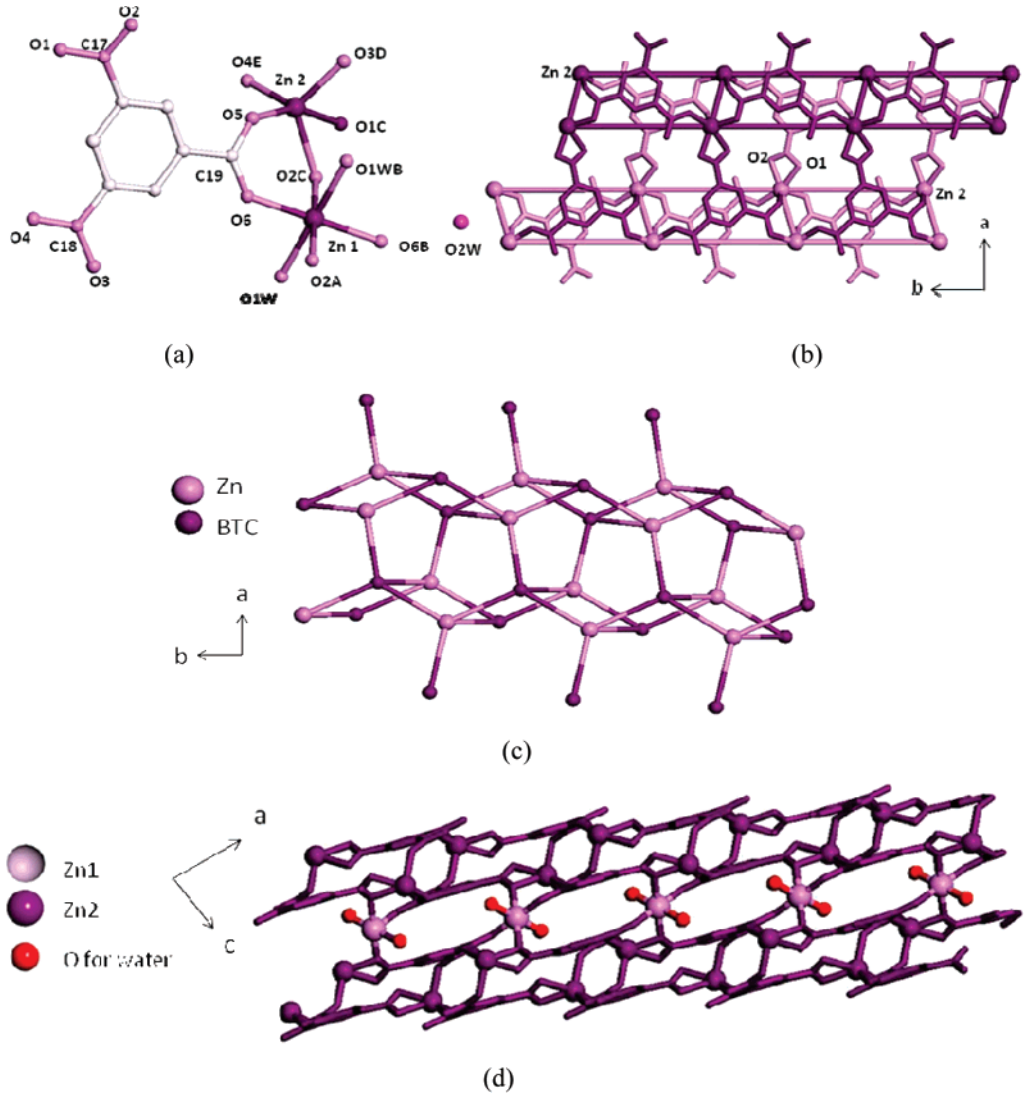


**Figure 2.** Structure of **2**: **(a)** Coordination environment of Zn. (b) The 2-D layer formed by linking the $[(Zn2)_4(BTC)_2]$ units with the water molecules being omitted for clarity. (c) The topological drawing of 2-D layer. (d) 3-D framework.

by five carboxylate oxygen atoms ($d_{Zn(2)-O}$ = 1.972(2)−2.239(2) Å) from four $BTC^{3-}$ ligands to display a distorted trigonal bipyramidal coordination environment with $\tau$ = 0.664 [$\tau = (\beta-\alpha)/60$, where $\alpha$ and $\beta$ are the two biggest bond angles around Zn center; $\tau$ = 0 for ideal square pyramid, and $\tau$ = 1 for ideal trigonal bipyramid],[16] which is different from the tetrahedron of Zn(2) in **1** (Figure 2a). Two $BTC^{3-}$ ligands link four Zn(2) atoms to form two kinds of 8- and 16-membered rings, whose linkage results in a ladder-like chain as that in **1**. However, the neighboring chains in **2** are antiparallel to each other, which is different from the parallel ones in **1** (Figure 1c and Figure 2c); these are further connected by Zn(2)−O(1) and Zn(2)−O(2) bonds into a 2-D layer (Figure 2b). These layers are linked through $Zn(1)O_6$ octahedra into a 3-D framework (Figure 2d). Water molecules O(2W) are located between the 2-D layers and form hydrogen bonds of O(2W)···O(1W) (3.079(1) Å). The neighboring phenyl rings in $BTC^{3-}$ ligands show both $\pi\cdots\pi$ interaction with the centroid-to-centroid distance 3.754 Å and d···$\pi$ interaction between C(14)-H and the phenyl ring with C(14)-to-centroid distance 3.387 Å.

Compound **3** was obtained from a $Zn^{2+}$-richest condition among the reactions performed in [EMI]Br (compounds **1**−**3**). Different from **1** and **2**, its crystal structure shows that $EMI^+$ cation functions as a template. Zn(1) atom is tetrahedrally coordinated by four carboxylic oxygen atoms ($d_{Zn(1)-O}$ = 1.814(2)−2.233(2) Å) from four $BTC^{3-}$ ligands (Figure 3a). The crystal structure can be described as stacking of puckered layers that are composed of eight-membered rings formed by two Zn atoms and two bridging bidentate $BTC^{3-}$ ligands and 32-membered rings formed by four Zn atoms and four $BTC^{3-}$ ligands between them in monodentate and bidentate modes. The 32-membered rings share common edges to form a 2-D layer and the eight-membered rings between them (Figure 3b). The layers are further bridged via Zn(1)−O(2) bonds with the $BTC^{3-}$ ligand displaying bidentate and bis-monodentate coordination modes to

(16) Addision, A. W.; Rao, T. N.; Reedijk, J.; Riju, J. V.; Verschoor, G. C. *J. Chem. Soc., Dalton Trans.* **1984**, 1349−1356.

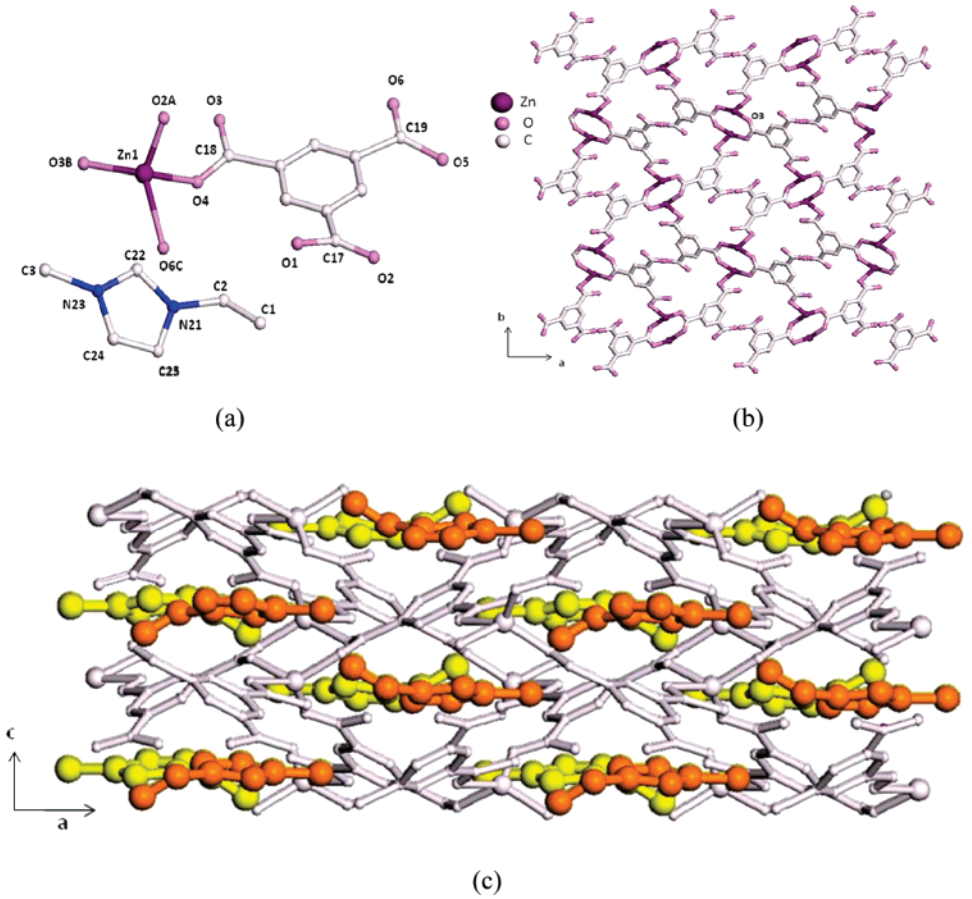


**Figure 3.** Structure of **3**: (a) Coordination environment of Zn. (b) The 2-D layer. (c) 3-D framework with EMI located in the channels (EMI are represented by yellow and orange colors).

form a 3-D framework. There are channels formed along the *b*-direction where the $EMI^+$ cations are located (Figure 3c).

The asymmetric unit of **4** contains one Zn atom, one $BTC^{3-}$ ligand, and one $PMI^+$. Zn(1) atom is coordinated with six oxygen atoms with three short ($d_{Zn(1)-O}$ = 2.015(2)−2.284(3) Å) and three long bonds ($d_{Zn(1)-O}$ = 2.568−2.763 Å) (Figure 4a). In fact, the latter three Zn−O bond distances are too long to be considered as normal coordination bonds. The valence sums of these three bonds total smaller than 0.1, almost negligible. Probably, the 3-D network structure of compound **4** exerts a matrix effect that keeps these oxygen atoms from coming closer, and the Zn(1) position is the energy minimum position under the restriction. The structure of **4** can be described as an interpenetration structure of two identical 3-D frameworks each constructed by enantiomeric pairs of two types of helices formed by $[Zn(BTC)]^-$ repeating units (Figure 4b and 4c). The two types of helices appear as a large 32-membered ring that surrounds $PMI^+$ ions and a small 16-membered ring in the view along the *a*-axis. The pitch height of these helices are *l* = 16.005 Å. The two types of helices are fused by sharing common edges composed of Zn and $BTC^{3-}$ into a 3-D framework structure. The interpenetration makes the pore rather small which is filled by $PMI^+$ ions (Figure 4d). The interaction between $PMI^+$ and the framework is electrostatic principally, but there also appears to be significant contribution from hydrogen bond of C(4)−H···O(11) (2.684(6) Å, 121.20°) between them. There is also a weak d···$\pi$ interaction between C(3)−H and the phenyl ring of $BTC^{3-}$ ($d_{C(3)-H\cdots centroid}$ = 3.594 Å, −C(3)−H−centroid = 118.17°).

There are four symmetry-independent Zn atoms and $BTC^{3-}$ ligands in **5** in the asymmetric unit (Figure 5a). Zn(1), Zn(2), and Zn(4) centers are in tetrahedra, and Zn(3) center is in an octahedron. O(1) acts as a $\mu_3$-bridge to connect Zn(1), Zn(2), and Zn(3) with Zn−O bond distances of 1.986(1), 1.994(1), and 2.148(1) Å, whose bond-valence sum is calculated to be 1.23 indicating that O(1) is $OH^-$; this assignment is in accord with the charge balance requirement. Both Zn(1) and Zn(2) atoms are surrounded by three carboxylic oxygen atoms from three $BTC^{3-}$ ligands ($d_{Zn(1)-O}$ = 1.940(1)−1.983(2) Å and $d_{Zn(2)-O}$ = 1.953(1)−1.982(1) Å) and O(1) from $OH^-$. On the other hand, all of the four oxygen atoms bonded to Zn(4) atom are from four different $BTC^{3-}$ ligands ($d_{Zn(4)-O}$ = 1.929(1)−1.967(1) Å). The octahedron around Zn(3) is formed by two carboxylic oxygen atoms ($d_{Zn(3)-O}$ = 2.127(1)−2.136(1) Å) from two $BTC^{3-}$ ligands located on axial positions, three ($d_{Zn(3)-O(1W)}$ = 2.048(1)−2.086(1) Å) and $OH^-$ lying in the equatorial plane. The three water molecules O(1W), O(2W), and O(3W) have bond-valence sum of 0.40, 0.39, and 0.36, suggesting that they are all neutral coordination water molecules.

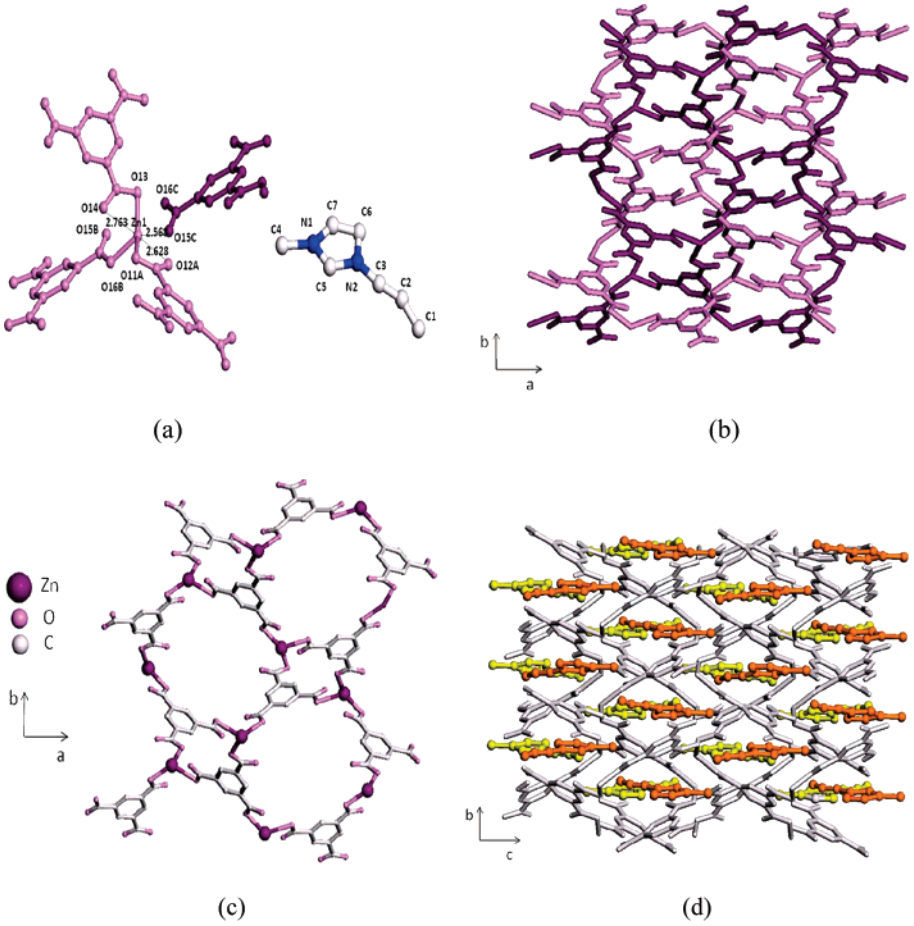


**Figure 4.** Structure of **4**: (a) Coordination environment of Zn. (b) A 3-D along *c* direction showing doubly interpenetrated frameworks (violet and pale violet color show each fragment). (c) One fragment of them along *c* direction. (d) Overall 3D framework generated with the PMI (orange and yellow) lied in the channels.

The structural description of **5** starts from a Zn(3)-BTC chain along the *a*-direction in which neighboring Zn(3) atoms are bridged by O(32) and O(33) atoms of $BTC^{3-}$. These chains are paired to form double chains through bridging Zn(4) atoms (Figure 5b), and the double chains are fused into a 2-D layer along the *ab* plane by bridging Zn(2) atoms through Zn(2)−O(14), Zn(2)−O(34), and Zn4−O11 bonds (Figure 5c). A rigid 3-D framework is constructed by several Zn−O bonds (Zn1−O1, O16, and O31; Zn3−O22; Zn4−O24) those link the 2-D layers (Figure 5d). The $BMI^+$ cation is located in the channels (Figure 5e), which interacts with the negatively charged framework. There are also two kinds of hydrogen bonds formed, the one between $BMI^+$ and O(25) (C(45)−H···O25 = 2.959(5) Å, 163.1°) Å and the other between water molecules and carboxylic oxygen atoms (O(1W)···O(21) = 2.650(2), O(2W)···O(12) = 2.697(2), O(2W)···O(23) = 2.747(2), O(2W)···O(3) = 3.064(2), O(3W)···O(13) = 2.814(2), O(3W)···O(26) = 2.780(2) Å).

Compound **6** distinguishes itself from the previous MOFs in that $Br^-$ constitutes the structure with Zn−Br bonds. As shown in Figure 6a, the asymmetric unit consists of two independent Zn atoms: Zn(1) is five-coordinated square pyramid $ZnO_5$ ($\tau$ = 0.375) and Zn(2) is four-coordinated distorted tetrahedron $ZnO_3Br$. There is a $\mu_3$-bridge oxygen O(1) that is bonded to Zn(1), Zn(1A) ($A = -x, 1 - y, 1 - z$) and Zn(2) with Zn−O bond distances of 2.024(9), 2.095 (9), and 1.944(9) Å. The calculated valence-sum for O(1) is 1.29, indicating that O(1) should be $OH^-$, which is in agreement with the charge balance consideration. Zn(1) is coordinated equatorially by two carboxylic oxygen atoms from two BTC ligands ($d_{Zn(1)-O(11)}$ = 1.994(9), $d_{Zn(1)-O(16)}$ = 2.074(1) Å) and two O(1) atoms of the $\mu_3$-$OH^-$ groups ($d_{Zn(1)-O(1)}$ = 2.024(9) and 2.095(9) Å) and axially by a carboxylic oxygen ($d_{Zn(1)-O(14)}$ = 2.017(1) Å). Zn(2) is coordinated by two carboxylic oxygen atoms ($d_{Zn(2)-O(12)}$ = 1.964(1), $d_{Zn(2)-O(15)}$ = 1.975(1) Å), O(1) and Br(1) ($d_{Zn(2)-Br(1)}$ = 2.321(3) Å). A $\mu_3$-$OH^-$ and its symmetry-related atom bridge four Zn atoms to form a subunit $[Zn_4(OH)_2Br_2]^{4-}$ with a crystallographic inversion center at the midpoint of Zn(1)···Zn(1A) (Figure 6b). By coordinating with Zn(1) and Zn(2A) by bidentate and with Zn(1A) by monodentate coordination modes, $BTC^{3-}$ ligands bridge the $[Zn_4(OH)_2Br_2]^{4-}$ subunits to form a 36-membered ring, whose expansion results in a 2-D layer. With the connection of Zn(1)−O(11) and Zn(2)−O(12), the 2-D layer is further grown into a 3-D framework with channels along the *a*-direction. $AMI^+$ cations are located between the layers (Figure 6c). The interaction between $AMI^+$ and the framework is solely electrostatic.

Omitting the guest IL cations, the void volumes of the MOFs were calculated to be 45.8% (**3**), 50.2% (**4**), 42.3%

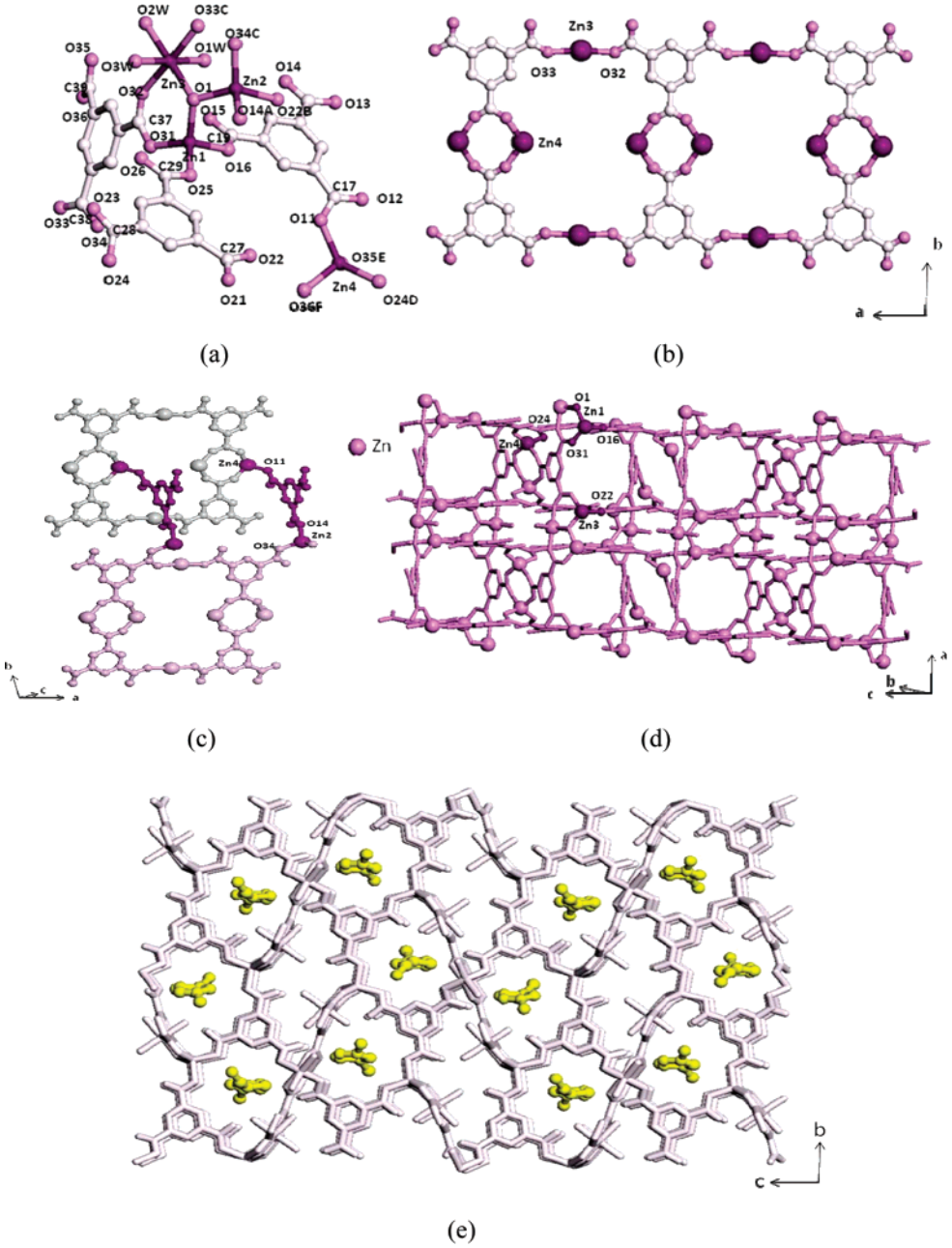


**Figure 5.** Structure of **5**: (a) Coordination environment of Zn. (b) The double chains formed from "Zn3-BTC chain" through bridging Zn4 atoms. (c) The extended 2-D layer formed by bridging Zn−O bonds. (d) 3-D framework omitted ILs $[BMI]^+$. (e) A view along *a* direction. EMI molecules as charge-compensating groups and template located in the channels and are represented by ball and stick model (yellow).

(**5**), and 54.0% (**6**) by PLATON.[17] One may notice that the trend of the void volume does not correlate with the size of the cations. In order to see the possibility of obtaining porous MOFs, we have attempted to exchange the organic cations with smaller ones such as $Na^+$ and $K^+$. However, in most of the cases we failed to find the right solvent in which the MOFs were stable or the ion-exchange reactions did not occur. The TG analyses of the six compounds indicate the skeletons of the frameworks and the ionic liquids decompose nearly synchronously, showing that the cations interact strongly with the frameworks, which appears to be the reason for the difficulties in our attempted ion-exchange reactions. Further studies on such possibilities are in progress.

In Table 2, we summarize some factors affecting the reaction system and resulting MOFs. Though we used the same reagents and reaction conditions, the six compounds show diverse structures. Even the coordination modes of $BTC^{3-}$ ligands are different. Although the systematic variation of the alkyl chain lengths of 1-alkyl-3-methylimidazolium bromide ILs may bring in systematic variations in the physical properties such as the melting point and viscosity, there are many other factors, such as solvent−solute and Zn−BTC interactions, which prohibit generalization. However,

(17) Spek, A. L. *Acta Crystallogr., Sect. A: Found. Crystallogr.* **1990**, *A46*, C43.

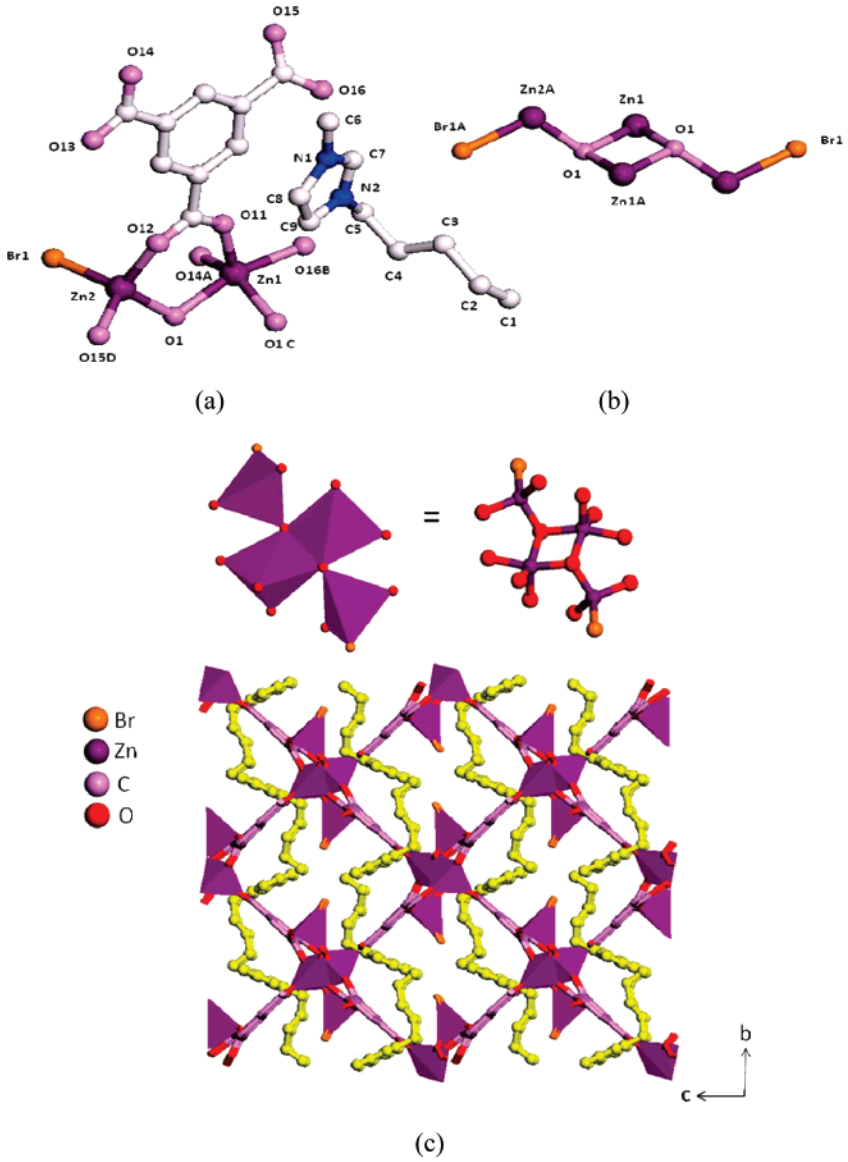


**Figure 6.** Structure of **6**: (a) The coordination spheres of Zn atoms. (b) The negative subunit $[Zn_4(OH)_2Br_2]^{4-}$. (c) 3-D framework generated with AMI (yellow) filled in the layers and the subunits $[Zn_4(OH)_2Br_2]^{4-}$ represented by polyhedron.

one may agree on that the imidazolium cations with longer chains have the tendency to be incorporated into the frameworks to result in through increased van der Waals interactions and that the EMI lies on the boundary between the templated and template-free MOFs.

## Conclusions

In this study, we have explored the ionothermal reaction systems between $Zn(NO_3)_2$ and $H_3BTC$ in a series of IL media. For this, we have employed four different 1-alkyl-3-methylimidazolium bromide ILs with the alkyl chain length varying from ethyl to amyl. Under the same reaction conditions except for the type of ILs and Zn:$H_3BTC$ ratios, we obtained six 3-D zinc MOFs with diverse features, including various coordination number of $Zn^{2+}$, the bonding modes of the BTC ligand from $\mu_3$ to $\mu_6$, and the role of the imidazolium cation in the final structures. Although the complex nature of the reaction systems prohibited any systemization of the resultant structures in relation with the ILs used, our results demonstrate the richness of the structural diversity of the ionothermal reaction systems in obtaining novel MOF compounds. Further investigation on such systems may yield many new MOF compounds with interesting features and useful properties. The tendency of high degree of condensation between $Zn^{2+}$ and $BTC^{3-}$ in **1**−**6** appears to be the feature relevant to the nature of the ionothermal reactions. Certainly, a large volume of experimental data needs to be accumulated for deeper understanding on the nature of ionothermal systems. Our present data and the few of works of the pioneering groups are just the beginning of such a paramount task.

**Acknowledgment.** This work was supported by the Korea Research Foundation Grant funded by the Korean Government (MOEHRD) (KRF-2005-005-J11903). We also thank CNNC and KOSEF for financial support.

**Supporting Information Available:** Crystallographic data, bond distances and angles, TG graphs, and observed and calculated XRPD patterns for compounds **1**−**6**, Zn−BTC compounds and coordination modes in the literatures. This material is available free of charge via the Internet at http://pubs.acs.org. Crystallographic data for **1**−**6** have been deposited at the Cambridge Crystallographic Data Center as supplementary publications (CCDC: 653389−653394). These data can be obtained free of charge at www.ccdc.cam.ac.uk/conts/retrieving.html (or from the CCDC, 12 Union Road, Cambridge CB2 1EZ, UK; fax: +441223336033; e-mail: deposit@ccdc.cam.ac.uk).

IC701393W